RESEARCH ARTICLE | SEPTEMBER 19 2023

Resistive switching localization by selective focused ion beam irradiation FREE

Nareg Ghazikhanian ; Javier del Valle ; Pavel Salev ; Ralph El Hage ; Yoav Kalcheim ; Coline Adda ; Ivan K. Schuller

Appl. Phys. Lett. 123, 123505 (2023)
https://doi.org/10.1063/5.0151823

Applied Physics Letters ARTICLE pubs.aip.org/aip/apl

Resistive switching localization by selective focused ion beam irradiation

Cite as: Appl. Phys. Lett. **123**, 123505 (2023); doi: 10.1063/5.0151823
Submitted: 24 March 2023 · Accepted: 3 September 2023 ·
Published Online: 19 September 2023

Nareg Ghazikhanian,[1,2,a)] Javier del Valle,[1,b)] Pavel Salev,[1,c)] Ralph El Hage,[1] Yoav Kalcheim,[1,d)] Coline Adda,[1] and Ivan K. Schuller[1,2]

AFFILIATIONS

[1]Department of Physics, University of California San Diego, 9500 Gilman Dr., La Jolla, California 92093, USA
[2]Program in Materials Science and Engineering, University of California San Diego, 9500 Gilman Dr., La Jolla, California 92093, USA

[a)]**Author to whom correspondence should be addressed:** nghazikh@ucsd.edu
[b)]**Present address:** Department of Physics, University of Oviedo, C/Federico García Lorca 18, 33007 Oviedo, Spain.
[c)]**Present address:** Department of Physics and Astronomy, University of Denver, 2199 S University Blvd., Denver, Colorado 80208, USA.
[d)]**Present address:** Department of Materials Science and Engineering, Technion - Israel Institute of Technology, Haifa 3200003, Israel.

ABSTRACT

Materials displaying resistive switching have emerged as promising candidates for implementation as components for neuromorphic computing. Under an applied electric field, certain resistive switching materials undergo an insulator-to-metal transition through the formation of a percolating filament, resulting in large resistance changes. The location and shape of these filaments are strongly influenced by hard-to-control parameters, such as grain boundaries or intrinsic defects, making the switching process susceptible to cycle-to-cycle and device-to-device variation. Using focused Ga^{+} ion beam irradiation, we selectively engineer defects in VO_2 and V_2O_3 thin films as a case study to control filament formation. Using defect pre-patterning, we can control the position and shape of metallic filaments and reduce the switching power significantly. A greater than three orders of magnitude reduction of switching power was observed in V_2O_3, and a less than one order of magnitude reduction was observed in VO_2. These experiments indicate that selective ion irradiation could be applied to a variety of materials exhibiting resistive switching and could serve as a useful tool for designing scalable, energy efficient circuits for neuromorphic computing.

Materials exhibiting resistive switching (RS) behavior have recently garnered much interest for nanoscale electronic devices. Particularly, RS materials could be implemented as components in innovative memories, selectors for ReRAM, optical switches, and artificial neurons and synapses for neuromorphic computing applications.[1–8] A wide variety of materials and mechanisms can give rise to RS, such as ionic drift,[9] crystallization/amorphization,[10,11] or a voltage-triggered insulator–metal transition.[12] Frequently, switching takes place through the formation of a conducting percolating filament within an otherwise insulating matrix.[13] A unique insulating barrier within a conducting matrix has also found in a complex oxide.[14] Device morphology often dictates switching characteristics, including the position, shape, and switching power necessary to induce a conducting filament. Due to nanoscale structural parameters, including grain sizes, local changes in stoichiometry, and intrinsic defects, many RS devices display large device-to-device variability.[15–17] Furthermore, inherent structural and electronic stochasticity at the nanoscale can also lead to cycle-to-cycle variability issues.[18]

A potential mitigation for variability problems might arise from locally altering the electronic properties of the devices to enable preferential location and shape of the filament formation. Lowering of threshold voltage and power for resistive switching in VO_2 has been achieved using various mechanisms, including doping, heat localization via carbon nano-tube incorporation, electron beam irradiation, and introduction of oxygen vacancies.[19–24] A comparison of voltage threshold reduction methods can be seen in supplementary material, Table S1. In addition to these methods, focused ion beam (FIB) irradiation is a particularly advantageous method for modifying global RS properties.[25–29] Due to the nature of the defects induced by ion irradiation, FIB has been demonstrated as a viable method of tuning

electronic properties in various material systems, resulting in changes in carrier concentration, mobility, and phase change behavior.[30,31] These changes have been observed within various materials and with irradiation of different ions over a wide range of energies,[30,32–34] implying that FIB irradiation could be a general and widely applicable method of tuning RS devices. In addition, FIB allows us to selectively create defects at the nanoscale by accurately controlling the irradiated area. In this paper, we show that FIB irradiation can be used to control the position and shape of filaments in both VO_2 and V_2O_3 microdevices. Importantly, we observe significant reduction in switching power, which could be attributed to a localization of Joule heating and a potential change in RS mechanism.

VO_2 and V_2O_3 are well-known correlated oxides featuring a first-order metal-insulator transition (MIT) at around 150 and 340 K, respectively.[35–37] Below the transition temperature, it is possible to electrically trigger partial metallization in the system. This happens through the formation of percolating metallic domains, which are arranged in a filamentary fashion and disappear when the voltage/current is removed, giving rise to volatile resistive switching.

VO_x thin films were grown via RF magnetron sputtering on (1 0 2)-oriented r-plane Al_2O_3 substrates. VO_2 thin films were deposited in a 3.6 mTorr Ar/O_2 (93/7%) atmosphere and at 470 °C substrate temperature by reactive RF magnetron sputtering from a V_2O_3 target. After growth, the VO_2 samples were maintained in the same atmosphere and cooled at a rate of 12 °C min^{-1}. For V_2O_3, the growth was done in a 7.9 mTorr Ar atmosphere and at 640 °C substrate temperature by RF magnetron sputtering from a V_2O_3 target. After the growth, the V_2O_3 samples were thermally quenched at a rate of ~90 °C min^{-1}, as this process helps to preserve the correct oxygen stoichiometry and allows for dramatic improvement of electronic properties.[38] X-ray diffraction characterization for both VO_2 and V_2O_3 films is shown in the supplementary material (Fig. S1). Resistance-temperature measurements revealed metal-insulator transitions, over five orders of magnitude resistance change at T_c ~160 K in V_2O_3 and over two orders of magnitude resistance change at T_c ~340 K in VO_2 [Figs. 1(c) and 1(d)], indicating the appropriate stoichiometry of synthesized films. After growth, two-terminal micro-gap geometries were fabricated via a combination of photolithography, e-beam evaporation of Au (100 nm)/Ti (20 nm) electrodes, and a liftoff process. VO_x devices were irradiated with an FEI Scios DualBeam focused ion beam scanning electron microscope using Ga^+ ions. The transport and switching characteristics of these samples were measured using a Keithley 2450 source measure unit (SMU).

Using FIB, we can control the MIT. Figure 1(a) shows a schematic representation of the vanadium oxide devices and measurement setup. Figure 1(b) shows a scanning electron microscope image of a two-terminal junction. A 1 μm wide strip of ion irradiation-induced defects spanning the entire length of the VO_x device can be seen at the edge of an otherwise pristine VO_x device. This discoloration could indicate the presence of locally induced defects that alter the intensity of detected secondary electrons emitted from the region. Figures 1(c) and 1(d) show resistance vs temperature measurements of V_2O_3 and VO_2 devices, respectively. The insulator-to-metal phase transition is readily observable for both materials. Several devices, with varying channel irradiation conditions, are shown. Each device has been exposed once using different irradiation conditions. For the V_2O_3 measurements, the charge per unit area was kept constant at 1 pC/μm^2 and the accelerating voltage was varied from 2 to 30 kV, as

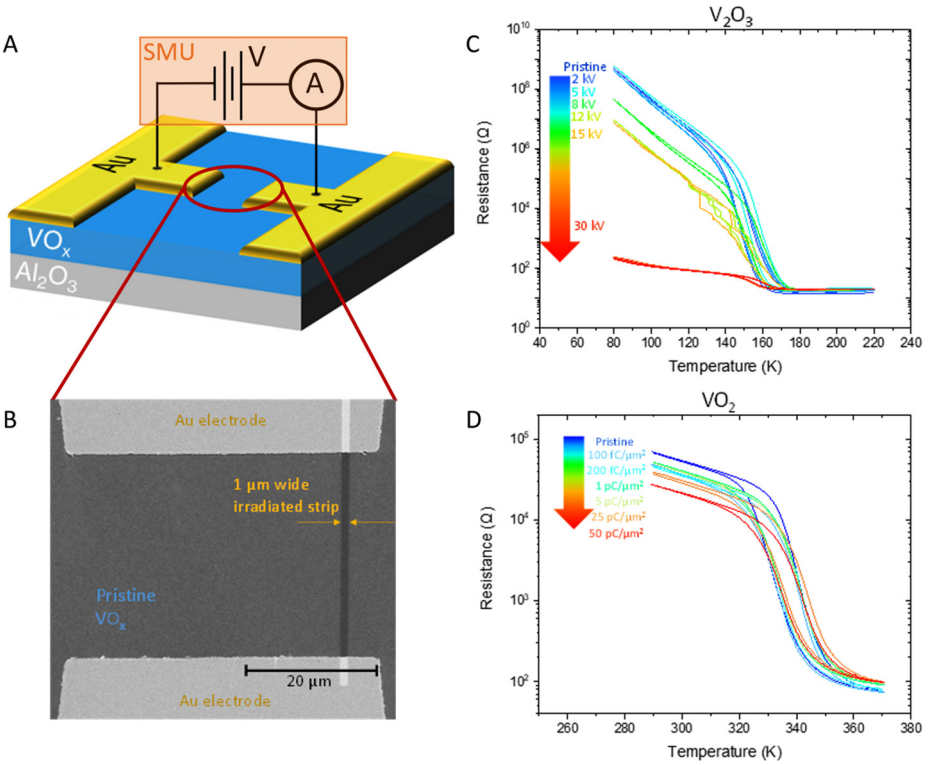

FIG. 1. (a) Schematic of voltage-controlled measurement setup for two-terminal resistive switching VO_x devices. (b) SEM image of a two-terminal V_2O_3 device with 1 μm wide irradiated path bridging the length of the device. (c) Resistance vs temperature measurements for a V_2O_3 device irradiated with varying doses 1 μm wide strips of Ga^+ ion irradiation. Accelerating voltage was varied as the transport properties of V_2O_3 are quite susceptible to change. All doses used 1 pC/um^2. (d) Resistance vs temperature measurements for VO_2 devices irradiated with varying doses of strips of Ga^+ ion irradiation. Beam current was varied as the transport properties of VO_2 are less susceptible to change upon irradiation, as compared to V_2O_3. All doses used the maximum accelerating voltage available to the system.

this allowed for a more refined control of the extent of defects induced. As VO_2 is much more robust against changes upon irradiation compared to V_2O_3 (Ref. 7), dose tests were performed by fixing the accelerating voltage at 30 kV and varying the charge per unit area from 100 fC/μm^2 to 50 pC/μm^2. We found that the FIB irradiation affects the insulating state resistance in both VO_2 and V_2O_3, as shown in the resistance–temperature plots, while the impact on the activation energy in the insulating state is minimal (supplementary material, Figs. S2 and S3). Overall, our measurements show that FIB is a flexible method to controllably induce defects either by using the irradiation dose in V_2O_3 or the accelerating voltage in VO_2. Since we locally altered the MIT, we can expect that there will be a change in local switching properties.

In V_2O_3, a qualitative change in the shape of the MIT arises in devices, which have been irradiated with a high enough accelerating voltage [curves for 12 and 15 kV in Fig. 1(c)]: the resistance of these devices changes in discrete, discontinuous jumps. These jumps most likely correspond to the nucleation of individual domains, as similar jumps have been observed in nanoscale devices where single domains dominate switching properties of the entire device.[16,39,40] For intermediate voltages, the effect is large enough to cause orders-of-magnitude change in the insulating state resistance of the device, yet not large enough to almost entirely suppress the MIT, as with the 30 kV case. Such qualitative changes are not apparent with irradiated VO_2 films, even at doses 50 times greater than those used to suppress the transition in V_2O_3 devices. It is noteworthy to mention that for doses larger than 50 pC/μm^2 at 30 kV, milling effects began to dominate over changes in material properties, as a significant percentage of the VO_x was milled away, leading to effectively different device geometries for the varying doses.

We found that local irradiation allows controlling the location and shape of the filament formation during resistive switching. Figure 2 shows images of conducting filaments formed during current-controlled RS in 2-terminal VO_2 and V_2O_3 devices, both before and after focused ion beam irradiation. These differential images are acquired via optical microscopy and processed by subtracting an image prior to applying current from an image of a device with a formed filament. Thus, the white regions represent the regions that have changed optically upon the application of 10 mA. This optical change corresponds to the local phase transition associated with RS.[41,42] Figure 2(a) shows a conducting filament in a pristine, 300 nm thick, 2-terminal VO_2 planar device, as well as a filament in the same device after it has been irradiated with a strip of Ga^+ ions. As expected,[43] the filament forms indiscriminately toward the center of the pristine device, the location of which is presumably dictated by inherent random defects that were introduced during the growth process. Furthermore, the filaments that form in the pristine devices form along a skewed angle due to herringbone pattern of the domains.[42,44] After patterning an irradiation strip on the right side of the device, the filament localizes in the irradiated region close to the right edge of the device along a straight path, overcoming the geometric constraints to both form diagonally and at the center of the device.[15,44] Figure 2(b) shows similar localization behavior in a 100 nm thick V_2O_3 device. In the pristine case, the filament forms on the left side of the device. After patterning an irradiation strip on the right side of the device, the filament localizes along the irradiated path. As this localization behavior is observed in two separate materials, it is possible that guiding filaments using FIB could be applied to many other materials.

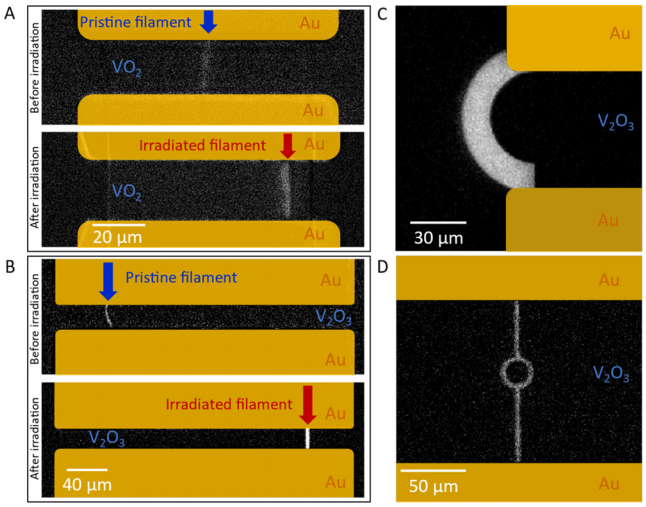

FIG. 2. (a) Differential images of conducting filaments in VO_2 before and after ion beam irradiation. The conducting filament localizes at the irradiated region. The device is 50 μm wide and 20 μm long. RS in the pristine device was performed at 320 and at 300 K after irradiation. (b) Differential images of conducting filaments in V_2O_3 before and after ion beam irradiation. The conducting filament localizes to the irradiated region. The device is 250 μm wide and 20 μm long. RS in the pristine device was performed at 141 and at 110 K after irradiation. (c) Differential image of conducting filament in V_2O_3 after ion beam irradiation. The conducting filament in 2 C localizes to the curved, irradiated region extending beyond the edge of the two-terminal device, overcoming geometric constraint. The gap width of the device is 60 μm. (d) Differential image of conducting filament in V_2O_3 after ion beam irradiation. Instead of forming along a linear path, the conducting filament splits and localizes along the curved irradiated region, overcoming geometric constraint. The gap width of the device is 100 μm. All images of filaments were acquired while applying 10 mA.

Additionally, FIB allows to guide the filament into more intricate shapes. Figure 2(c) shows a conducting filament that has formed along a curved irradiated pattern beyond the edges of the electrodes. Figure 2(d) shows a conducting filament that has formed along a circular irradiated pattern. Rather than forming along a linear direct path, the filament splits and forms along both sides of a longer circular pattern. The ability to control the filament's location and shape allows for tuning resistive switching properties, a distinctive feature that could find applications in oxide electronics.

By localizing the filament, we can dramatically reduce switching power. Figure 3 shows voltage-controlled I–V measurements for both 10 nm thick, 10 μm V_2O_3 devices, and 100 nm thick, 10 × 40 μm^2 VO_2 devices. We note that the recorded voltage-controlled I–V curves show abrupt switching (i.e., sudden jumps in the I–V curves) instead of the development of a gradual negative differential resistance region that is commonly observed in the current controlled I–V measurements.[45,46] Figure 3 also shows cycle-to-cycle switching power variation statistics of the power necessary to induce RS in the same device over numerous cycles. The switching power was calculated as the current–voltage product at the point where an individual I–V curve exhibited an abrupt jump, i.e., the switching from the insulating to metallic state. The statistics were acquired over 100 switching cycles in a single device both before and after irradiation. No load resistors were used, and the same circuit configuration was used for all I–V

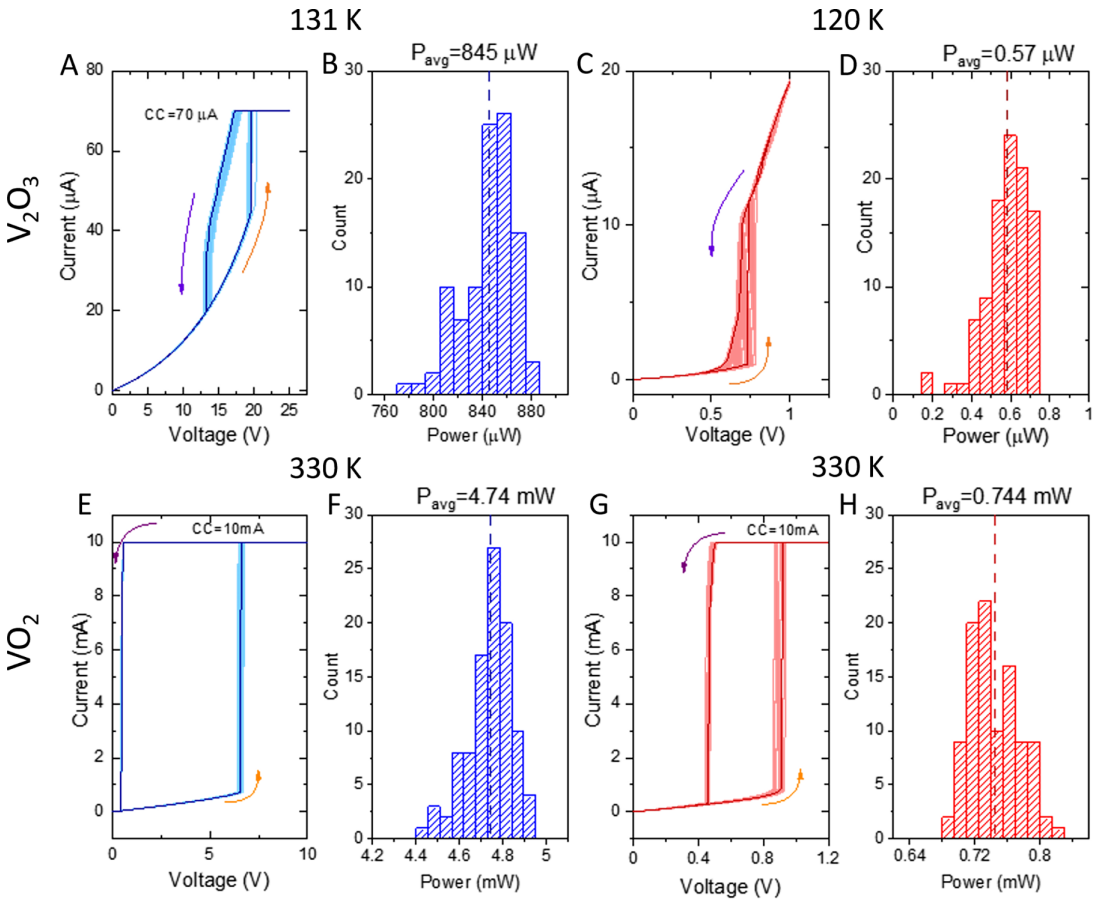

FIG. 3. (a) and (e) Voltage-controlled RS measurements in pristine V_2O_3 and VO_2 over 100 switching cycles, respectively. (b) and (f) show histograms of switching power for the respective data shown in Figs. 3(a) and 3(e), corresponding to the formation of a conducting filament (orange arrow). (c) and (g) 100 cycles of voltage-controlled RS measurements for the same devices measured in Figs. 3(a) and 3(e) after a 1 μm wide strip of gallium ion irradiation. Note that after irradiating the V_2O_3 device, the switching voltage is reduced by a factor of ~20 and the I–V curve is below current compliance after switching [panel (c)]. (d) and (h) Histograms of switching power for the respective data shown in Figs. 3(c) and 3(g), corresponding to the formation of a conducting filament (orange arrow).

measurements. Figures 3(a) and 3(e) (in blue) show I–V measurements for pristine V_2O_3 and VO_2, respectively. The dark blue curves show a single switching cycle, while the lighter blue curves show all subsequent cycles. Figures 3(b) and 3(f) (also in blue), thus, show average switching power statistics in pristine devices. Figures 3(c) and 3(g) (in red) show that 100 cycles of RS after the same devices in Figs. 3(a) and 3(e) had been irradiated with 1 μm wide strips of Ga^+ irradiation. The doses used for both the V_2O_3 and VO_2 devices were 1 pC/μm^2 at 16 keV accelerating voltage. The darker red curves delineate a single switching cycle while the paler red shows subsequent cycles. Figures 3(d) and 3(h) are the resultant histograms of switching power after irradiation.

For the V_2O_3 device, a drastic change in switching power can be observed upon irradiation. The average switching power in this device is reduced by over three orders of magnitude, changing from 845 μW in the pristine state to 0.57 μW after irradiation. The RS measurements were performed at 131 K before irradiation and at 120 K after irradiation, due to the shift in T_c. After irradiation, the RS measurement was chosen to be performed at 120 K to reproduce the same initial resistance as in the pristine device measurements. For measurements in both pristine and irradiated devices, the current compliance of the SMU was set to 70 μA so as to minimize current surges from the voltage source, which could lead to nonvolatile degradation of the device. After irradiation, a two orders of magnitude reduction in absolute cycle-to-cycle variability was observed.

For the VO_2 device, a less pronounced effect is observed, with a sixfold reduction in switching power from 4.74 to 0.74 mW, on average. As there was no shift in T_c for VO_2, the pristine and irradiated RS measurements were performed at the same temperature of 330 K. The current compliance of the SMU was set to 10 mA to minimize current spikes that could lead to nonvolatile degradation of the device. Even though the power reduction in VO_2 was much lower as compared to that of V_2O_3, we were still able to localize the filament by irradiation. This suggests that irradiation can be effective even in materials those are not very susceptible to ion irradiation induced defects. Furthermore, this indicates that it is not necessary to use comparatively high doses to achieve filament localization, as even low doses of irradiation induced defects are sufficient to guide the filament.

A switching power reduction using electron beam irradiation (as opposed to the ion beam irradiation in this work) has been reported in VO_2 devices.[23] The effect of the electron beam irradiation, however, was found to reverse upon exposing the sample to atmosphere. On the contrary, we found that the ion beam irradiation induced permanent changes both in VO_2 and V_2O_3. We did not observe recovery of the pristine properties after atmosphere exposure, voltage and thermal cycling, or prolonged storage. Therefore, the electron and ion beam irradiation provide different tool sets to control the switching properties in the MIT-based devices.

Our results can be understood considering filament formation dynamics. Filaments have been shown to be initiated by hotspots and to grow from them.[47–49] Joule heating can often drive the switching behavior in MIT materials.[48,50,51] By irradiating our devices, we are providing the sample with a preferential area where local resistance is lower [see Figs. 1(c) and 1(d)], which dominates current conduction. As a result, Joule heating is higher in this region, which helps to induce a local hotspot. As current flows more uniformly in a pristine device, higher current is needed to warm up a larger volume of material. Thus, higher current is needed to warm potential hotspots close to the transition temperature to induce RS. On the contrary, in irradiated devices, the resistivity of the irradiated areas is already low without any current applied due to the FIB-induced suppression of the MIT, and these areas will focus the current and initiate filament formation with lower total current. It has been shown in the literature that increasing defect concentrations in vanadium oxides can induce hopping-like conductivity and facilitate field-induced doping, which can lead to a non-thermal MIT.[31,52]

In conclusion, we showed that selective defect engineering using focused ion beam irradiation of VO_2 and V_2O_3 can both localize the electrically triggered phase transition and significantly reduce the switching power necessary to do so. The metal-insulator transition in V_2O_3 is often considered a primarily Mott type transition[53] and is quite susceptible to irradiation while evidence would suggest that VO_2 is a Peierls type transition.[54] As this effect was observed in various resistive switching materials displaying different physics, it is likely that such a process could be applied to various other material systems. This localization and reduction in switching power lend well to design and implementation of future micro- and nano-scale structures. By controlling the local conductance in an otherwise insulating matrix, it could be possible to implement various types of devices in the same material, a potentially worthwhile prospect for neuromorphic computing applications. Furthermore, the reduced switching power and confinement of filament formation in irradiated devices could allow for design of smaller and more energy efficient devices, which suits well for scalability considerations. Moreover, the overall width of the switching distribution [Figs. 3(d) and 3(h)] being narrower in irradiated samples implies that this method could reduce device-to-device and cycle-to cycle-variability in switching devices. Additionally, localized irradiation modification could be induced using shadow masks and global irradiation, enabling larger scale and faster device implementation. The experiments presented in this paper focused on controlling volatile RS, yet it is possible such irradiation techniques could be applied to materials displaying nonvolatile RS behavior. Often, the mechanisms of these nonvolatile resistive switching systems involve ionic migration, which is also strongly dependent on the morphological properties of the insulating film.[55–57] It is, therefore, feasible to achieve similar localization in nonvolatile RS materials by creating preferred drift channels, as it has already been shown that defect engineering can reduce cycle-to-cycle variation in such systems.[58]

See the supplementary material for x-ray characterization, analysis regarding transition activation energies, and comparisons to other voltage threshold reduction methods reported in VO_2 referenced in this work.

This work was supported by the Air Force Office of Scientific Research under Award No. FA9550-22-1-0135. Device fabrication and irradiation were carried out at the NANO3 cleanroom facility at UC San Diego.

AUTHOR DECLARATIONS

Conflict of Interest

The authors have no conflicts to disclose.

Author Contributions

Nareg Ghazikhanian: Conceptualization (lead); Data curation (lead); Formal analysis (lead); Funding acquisition (supporting); Investigation (lead); Methodology (lead); Project administration (lead); Resources (lead); Software (lead); Supervision (lead); Validation (lead); Visualization (lead); Writing – original draft (lead); Writing – review & editing (lead). **Javier del Valle:** Conceptualization (equal); Data curation (equal); Formal analysis (equal); Investigation (equal); Methodology (equal); Project administration (equal); Resources (equal); Supervision (equal); Validation (equal); Visualization (equal); Writing – review & editing (equal). **Pavel Salev:** Data curation (equal); Formal analysis (equal); Investigation (equal); Software (equal); Validation (equal); Visualization (equal); Writing – review & editing (equal). **Ralph El Hage:** Data curation (equal); Formal analysis (equal); Investigation (equal); Validation (equal); Visualization (equal); Writing – review & editing (equal). **Yoav Kalcheim:** Conceptualization (equal); Investigation (equal); Methodology (equal); Supervision (equal); Writing – review & editing (equal). **Coline Adda:** Formal analysis (equal); Software (equal); Validation (equal); Visualization (equal); Writing – review & editing (equal). **Ivan K. Schuller:** Conceptualization (equal); Funding acquisition (lead); Project administration (lead); Resources (lead); Supervision (lead); Writing – review & editing (equal).

DATA AVAILABILITY

The data that support the findings of this study are available from the corresponding author upon reasonable request.

REFERENCES

[1]Z. Yang, C. Ko, and S. Ramanathan, Annu. Rev. Mater. Res. **41**(1), 337 (2011).
[2]P. Stoliar, J. Tranchant, B. Corraze, E. Janod, M.-P. Besland, F. Tesler, M. Rozenberg, and L. Cario, Adv. Funct. Mater. **27**(11), 1604740 (2017).
[3]N. Shukla, A. V. Thathachary, A. Agrawal, H. Paik, A. Aziz, D. G. Schlom, S. K. Gupta, R. Engel-Herbert, and S. Datta, Nat. Commun. **6**(1), 7812 (2015).
[4]S. Kumar, J. P. Strachan, and R. S. Williams, Nature **548**(7667), 318 (2017).
[5]H. Jerominek, F. Picard, and D. Vincent, Opt. Eng. **32**(9), 2092 (1993).
[6]T. Driscoll, H. T. Kim, B. G. Chae, M. Di Ventra, and D. N. Basov, Appl. Phys. Lett. **95**(4), 043503 (2009).

[7]J. del Valle, P. Salev, Y. Kalcheim, and I. K. Schuller, Sci. Rep. **10**(1), 4292 (2020).
[8]S.-H. Bae, S. Lee, H. Koo, L. Lin, B. H. Jo, C. Park, and Z. L. Wang, Adv. Mater. **25**(36), 5098 (2013).
[9]R. Waser and M. Aono, Nat. Mater. **6**(11), 833 (2007).
[10]H. S. P. Wong, S. Raoux, S. Kim, J. Liang, J. P. Reifenberg, B. Rajendran, M. Asheghi, and K. E. Goodson, Proc. IEEE **98**(12), 2201 (2010).
[11]W. Zhang, R. Mazzarello, M. Wuttig, and E. Ma, Nat. Rev. Mater. **4**(3), 150 (2019).
[12]J. Duchene, M. Terraillon, P. Pailly, and G. Adam, Appl. Phys. Lett. **19**(4), 115 (1971).
[13]T. Luibrand, A. Bercher, R. Rocco, F. Tahouni-Bonab, L. Varbaro, C. W. Rischau, C. Domínguez, Y. Zhou, W. Luo, S. Bag, L. Fratino, R. Kleiner, S. Gariglio, D. Koelle, J.-M. Triscone, M. J. Rozenberg, A. B. Kuzmenko, S. Guénon, and J. del Valle, Phys. Rev. Res. **5**(1), 013108 (2023).
[14]P. Salev, L. Fratino, D. Sasaki, R. Berkoun, J. del Valle, Y. Kalcheim, Y. Takamura, M. Rozenberg, and I. K. Schuller, Nat. Commun. **12**(1), 15499 (2021).
[15]A. G. Shabalin, J. Valle, N. Hua, M. J. Cherukara, M. V. Holt, I. K. Schuller, and O. G. Shpyrko, Small **16**(50), 2005439 (2020).
[16]J. del Valle, J. G. Ramírez, M. J. Rozenberg, and I. K. Schuller, J. Appl. Phys. **124**(21), 211101 (2018).
[17]J. del Valle, Y. Kalcheim, J. Trastoy, A. Charnukha, D. N. Basov, and I. K. Schuller, Phys. Rev. Appl. **8**(5), 054041 (2017).
[18]S. Cheng, M.-H. Lee, R. Tran, Y. Shi, X. Li, H. Navarro, C. Adda, Q. Meng, L.-Q. Chen, R. C. Dynes, S. P. Ong, I. K. Schuller, and Y. Zhu, Proc. Natl. Acad. Sci. U. S. A. **118**(37), e2105895118 (2021).
[19]J. Zhang, Z. Zhao, J. Li, H. Jin, F. Rehman, P. Chen, Y. Jiang, C. Chen, M. Cao, and Y. Zhao, ACS Appl. Mater. Interfaces **9**(32), 27135 (2017).
[20]M. Pattanayak, M. N. F. Hoque, Y.-C. Ho, W. Li, Z. Fan, and A. A. Bernussi, Appl. Mater. Today **30**, 101642 (2023).
[21]S. M. Bohaichuk, M. Muñoz Rojo, G. Pitner, C. J. McClellan, F. Lian, J. Li, J. Jeong, M. G. Samant, S. S. Parkin, and H.-S. P. Wong, ACS Nano **13**(10), 11070 (2019).
[22]B. Wang, R. Peng, X. Wang, Y. Yang, E. Wang, Z. Xin, Y. Sun, C. Li, Y. Wu, and J. Wei, ACS Nano **15**(6), 10502 (2021).
[23]M. Belyaev, A. Velichko, V. Putrolaynen, V. Perminov, and A. Pergament, Phys. Status Solidi C **14**(3–4), 1600236 (2017).
[24]R. Naik B, D. Verma, and V. Balakrishnan, Appl. Phys. Lett. **120**(6), 062101 (2022).
[25]X. Xiang, Z. He, J. Rao, Z. Fan, X. Wang, and Y. Chen, ACS Appl. Electron. Mater. **3**(3), 1031 (2021).
[26]J. G. Ramirez, T. Saerbeck, S. Wang, J. Trastoy, M. Malnou, J. Lesueur, J.-P. Crocombette, J. E. Villegas, and I. K. Schuller, Phys. Rev. B **91**(20), 205123 (2015).
[27]J. Trastoy, C. Ulysse, R. Bernard, M. Malnou, N. Bergeal, J. Lesueur, J. Briatico, and J. E. Villegas, Phys. Rev. Appl. **4**(5), 054003 (2015).
[28]J. Valles, Jr., A. White, K. Short, R. Dynes, J. Garno, A. Levi, M. Anzlowar, and K. Baldwin, Phys. Rev. B **39**(16), 11599 (1989).
[29]J. Lesueur, L. Dumoulin, S. Quillet, and J. Radcliffe, J. Alloys Compd. **195**, 527 (1993).
[30]H. Mei, A. Koch, C. Wan, J. Rensberg, Z. Zhang, J. Salman, M. Hafermann, M. Schaal, Y. Xiao, R. Wambold, S. Ramanathan, C. Ronning, and M. A. Kats, Nanophotonics **11**(17), 3923 (2022).
[31]Y. Kalcheim, A. Camjayi, J. del Valle, P. Salev, M. Rozenberg, and I. K. Schuller, Nat. Commun. **11**(1), 2985 (2020).
[32]J. Trastoy, A. Camjayi, J. del Valle, Y. Kalcheim, J. P. Crocombette, D. A. Gilbert, J. A. Borchers, J. E. Villegas, D. Ravelosona, M. J. Rozenberg, and I. K. Schuller, Phys. Rev. B **101**(24), 245109 (2020).
[33]H. Hofsäss, P. Ehrhardt, H. G. Gehrke, M. Brötzmann, U. Vetter, K. Zhang, J. Krauser, C. Trautmann, C. Ko, and S. Ramanathan, AIP Adv. **1**(3), 032168 (2011).
[34]J. Rensberg, S. Zhang, Y. Zhou, A. S. McLeod, C. Schwarz, M. Goldflam, M. Liu, J. Kerbusch, R. Nawrodt, S. Ramanathan, D. N. Basov, F. Capasso, C. Ronning, and M. A. Kats, Nano Lett. **16**(2), 1050 (2016).
[35]F. J. Morin, Phys. Rev. Lett. **3**(1), 34 (1959).
[36]J. H. Park, J. M. Coy, T. S. Kasirga, C. Huang, Z. Fei, S. Hunter, and D. H. Cobden, Nature **500**(7463), 431 (2013).
[37]M. Imada, A. Fujimori, and Y. Tokura, Rev. Mod. Phys. **70**(4), 1039 (1998).
[38]J. Trastoy, Y. Kalcheim, J. del Valle, I. Valmianski, and I. K. Schuller, J. Mater. Sci. **53**(12), 9131 (2018).
[39]S. Wang, J. G. Ramírez, and I. K. Schuller, Phys. Rev. B **92**(8), 085150 (2015).
[40]A. Sharoni, J. G. Ramírez, and I. K. Schuller, Phys. Rev. Lett. **101**(2), 026404 (2008).
[41]A. S. McLeod, E. Van Heumen, J. G. Ramirez, S. Wang, T. Saerbeck, S. Guenon, M. Goldflam, L. Anderegg, P. Kelly, A. Mueller, M. K. Liu, I. K. Schuller, and D. N. Basov, Nat. Phys. **13**(1), 80 (2017).
[42]M. Lange, S. Guénon, Y. Kalcheim, T. Luibrand, N. M. Vargas, D. Schwebius, R. Kleiner, I. K. Schuller, and D. Koelle, Phys. Rev. Appl. **16**(5), 054027 (2021).
[43]I. Valmianski, P. Y. Wang, S. Wang, J. G. Ramirez, S. Guénon, and I. K. Schuller, Phys. Rev. B **98**(19), 195144 (2018).
[44]S. Cheng, M.-H. Lee, X. Li, L. Fratino, F. Tesler, M.-G. Han, J. del Valle, R. C. Dynes, M. J. Rozenberg, I. K. Schuller, and Y. Zhu, Proc. Natl. Acad. Sci. U. S. A. **118**(9), e2013676118 (2021).
[45]A. Crunteanu, J. Givernaud, J. Leroy, D. Mardivirin, C. Champeaux, J.-C. Orlianges, A. Catherinot, and P. Blondy, Sci. Technol. Adv. Mater. **11**(6), 065002 (2010).
[46]B. K. Ridley, Proc. Phys. Soc. **82**(6), 954 (1963).
[47]A. Zimmers, L. Aigouy, M. Mortier, A. Sharoni, S. Wang, K. G. West, J. G. Ramirez, and I. K. Schuller, Phys. Rev. Lett. **110**(5), 056601 (2013).
[48]S. Kumar, M. D. Pickett, J. P. Strachan, G. Gibson, Y. Nishi, and R. S. Williams, Adv. Mater. **25**(42), 6128 (2013).
[49]C. Adda, M.-H. Lee, Y. Kalcheim, P. Salev, R. Rocco, N. M. Vargas, N. Ghazikhanian, C.-P. Li, G. Albright, M. Rozenberg, and I. K. Schuller, Phys. Rev. X **12**(1), 011025 (2022).
[50]S. Slesazeck, H. Mähne, H. Wylezich, A. Wachowiak, J. Radhakrishnan, A. Ascoli, R. Tetzlaff, and T. Mikolajick, RSC Adv. **5**(124), 102318 (2015).
[51]N. Shukla, T. Joshi, S. Dasgupta, P. Borisov, D. Lederman, and S. Datta, Appl. Phys. Lett. **105**(1), 012108 (2014).
[52]D. Wickramaratne, N. Bernstein, and I. Mazin, Phys. Rev. B **99**(21), 214103 (2019).
[53]S. Lupi, L. Baldassarre, B. Mansart, A. Perucchi, A. Barinov, P. Dudin, E. Papalazarou, F. Rodolakis, J. P. Rueff, J. P. Itié, S. Ravy, D. Nicoletti, P. Postorino, P. Hansmann, N. Parragh, A. Toschi, T. Saha-Dasgupta, O. K. Andersen, G. Sangiovanni, K. Held, and M. Marsi, Nat. Commun. **1**(1), 105 (2010).
[54]S. Biermann, A. Poteryaev, A. I. Lichtenstein, and A. Georges, Phys. Rev. Lett. **94**(2), 026404 (2005).
[55]Y. Yang, P. Gao, S. Gaba, T. Chang, X. Pan, and W. Lu, Nat. Commun. **3**(1), 732 (2012).
[56]R. Waser, R. Dittmann, G. Staikov, and K. Szot, Adv. Mater. **21**(25–26), 2632 (2009).
[57]J. J. Yang, D. B. Strukov, and D. R. Stewart, Nat. Nanotechnol. **8**(1), 13 (2013).
[58]Z. J. Tan, V. Somjit, C. Toparli, B. Yildiz, and N. Fang, Phys. Rev. Mater. **6**(10), 105002 (2022).